

Some current observations near the continental slope off Portugal

by

J. MEINCKE, G. SIEDLER and W. ZENK, Institut für Meereskunde, Kiel

With 10 figures and 4 tables

Einige Strömungsbeobachtungen nahe am Kontinentalabfall vor Portugal

Zusammenfassung

Es werden einige Strommesserdaten dargestellt, die mit einer Verankerung auf 2450 m Wassertiefe nahe am Kontinentalrand vor Portugal erhalten wurden. Die mittleren Strömungen sind in allen fünf Beobachtungstiefen nordwärts gerichtet. Die Beiträge der mittleren Geschwindigkeiten liegen im Kern des Mittelmeerwassers um 2 bis 3 cm/sec höher als in geringeren Tiefen; das deutet auf eine Advektion dieser speziellen Wassermassen hin. Beim zeitlich veränderlichen Anteil der Strömungen überwiegen halbtägige Gezeiten. Die Entwicklung nach Eigenfunktionen zeigt ein Überwiegen des baroklinen Anteiles 2. Ordnung. Er trägt mit 48% zur horizontalen kinetischen Energie des Gezeitenstromes bei. Die Ergebnisse zum barotropen Anteil stimmen mit früheren Vorhersagen für dieses Gebiet überein. Die Bewegungen mit Kreisfrequenz ω im Interne-Schwere-Wellen-Band lassen sich gut durch ein Potenzgesetz der Form ω^{-2} für das Energiedichtespektrum beschreiben. Dieses Ergebnis steht in Übereinstimmung mit früheren Beobachtungen in anderen Meeresgebieten.

Summary

Some current meter data obtained from a mooring at 2450 m water depth near the continental slope off Portugal are presented. The mean currents at five levels with observations are northward. Mean speeds in the core of the Mediterranean Water exceed speeds at shallower levels by 2 to 3 cm/sec, indicating advection connected to this specific water mass. The current variability is dominated by semi-diurnal tidal components. Normal mode analysis

reveals a predominant mode of order 2, representing 48% of the total kinetic tidal energy. Results for the barotropic tidal component are in good agreement with earlier predictions for this area. The motion at higher frequencies ω in the internal gravity wave band can be well described by a ω^{-2} power law for the energy density spectrum. This result is consistent with earlier observations in other parts of the ocean.

1 Introduction

The current data presented in this paper result from an investigation of the Mediterranean outflow water in the area west of Gibraltar during "Meteor" cruise no. 8 in 1967 (CLOSS et al. 1969). The hydrographic data from this cruise have been discussed earlier by SIEDLER (1967), GIESKES et al. (1970) and ZENK (1970, 1971). Moored current meters had been placed at two positions on the Ibero-Moroccan shelf and at one position near the continental slope off Portugal. A paper by SIEDLER et al. (1974) dealt with the current data obtained on the shelf. The following discussion is restricted to the results obtained from the deep-water mooring off Portugal.

2 The observations

The mooring was launched on 13 February 1967 at the position $\Phi = 37^{\circ} 00' N$, $\lambda = 09^{\circ} 53' W$ at a depth of 2450 m. The mooring location and design are presented in figs. 1 and 2. Six current meters of the Richardson type and one temperature-pressure recorder were placed at different depth levels on a subsurface mooring line. Buoyancy packages consisting of aluminium or plastic net balls were distributed along the line. To obtain back-up

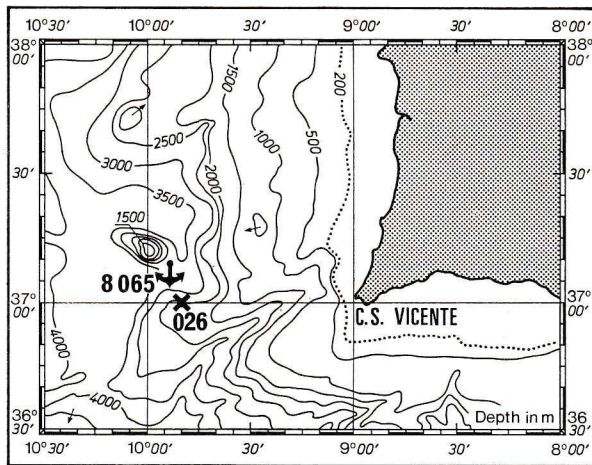


Fig. 1. Location of mooring no. 026 and "Meteor" anchor station no. 8065.

Abb. 1. Lage der Verankerung Nr. 026 und der „Meteor“ Ankerstation Nr. 8065.

methods for recovery in addition to the timed release operated surfacing float, a ground-line mooring and a surface buoy were included. The additional radar reflector buoy was attached to the radio buoy some time after the launching as a navigational aid for the research vessel's operations. The mooring was retrieved successfully with the normal mode of recovery on 25 February 1967.

A summary of the current time series obtained is given in table 1. As can be seen from the comments, all the instruments failed to operate properly due to various reasons. Nevertheless, usable records could be obtained from five instruments. A special problem was posed by the missing vane data of two meters. It was assumed here that the housing orientation could be used as a direction signal. The housings had fins attached to them. The gross features of the data obtained in this way from these two instruments are very similar to those at shallower and deeper levels:

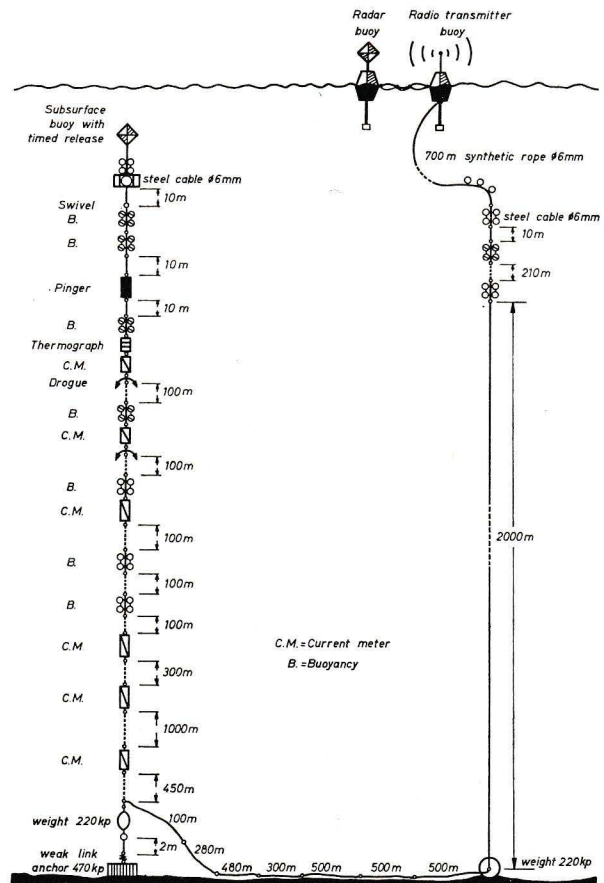


Fig. 2. Mooring design.

Abb. 2. Skizze des verankerten Meßsystems.

A rather steady flow is observed with variable currents superimposed which are usually smaller in magnitude, thus resulting in small directional variability. The above assumption therefore appears reasonable.

A further remark on the quality of the current meter data is concerned with the motions of the mooring system. The pressure recorder just above

Table 1
Tabelle 1

Summary of the current time series obtained from mooring 026
Überblick über die Zeiterien der Strömungsdaten von Verankerung 026

Reference No.	Depth (m)	Sampling interval (min)	Start of usable record	End of usable record	Comments
026101	234	5	04.15, 14. 2. 67 (GMT)	01.45, 21. 2. 67	At first good record, then loss of rotor magnets
026102	337	5	14.40, 13. 2. 67	08.45, 25. 2. 67	Vane was stuck
026103	440	20	14.15, 13. 2. 67	03.45, 20. 2. 67	Poor read pulses, but usable record
026104	744	5	14.20, 13. 2. 67	10.05, 25. 2. 67	At first good record, then loss of 1 rotor magnet
026105	1045	5	—	—	No record, clock failed
026106	2046	5	14.25, 13. 2. 67	09.45, 19. 2. 67	Vane was stuck, later failure of film advance

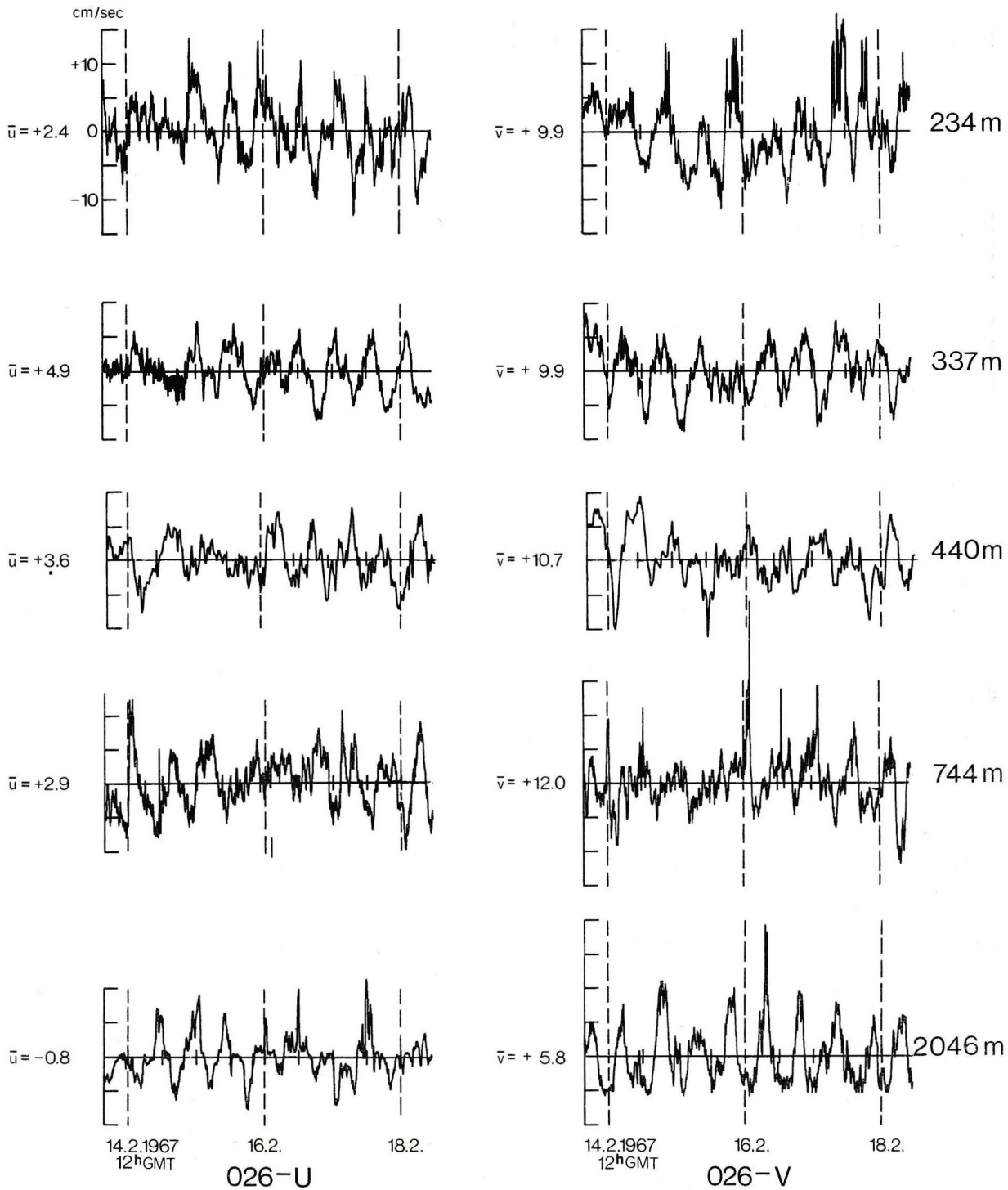


Fig. 3. Time series of east-west (u) and north-south (v) current components for selected period of simultaneous records. Mean currents are subtracted and indicated on the left side.

Abb. 3. Zeitserien der Ost-West (u)- und Nord-Süd (v)-Komponenten des Stroms für einen ausgewählten Zeitraum mit gemeinsamer Registrierung. Mittlere Ströme sind subtrahiert und links angegeben.

the uppermost current meter at a depth of 233 m did not show variations within its resolution of ± 10 dbar. There is however no information on accelerations and inclinations of the system. Nevertheless it seems justified to state that the error

induced by mooring motions is negligible for the type of analysis carried out in this paper.

The time series of the east-west (u) and north-south (v) components are presented in fig. 3. The mean current was subtracted before plotting,

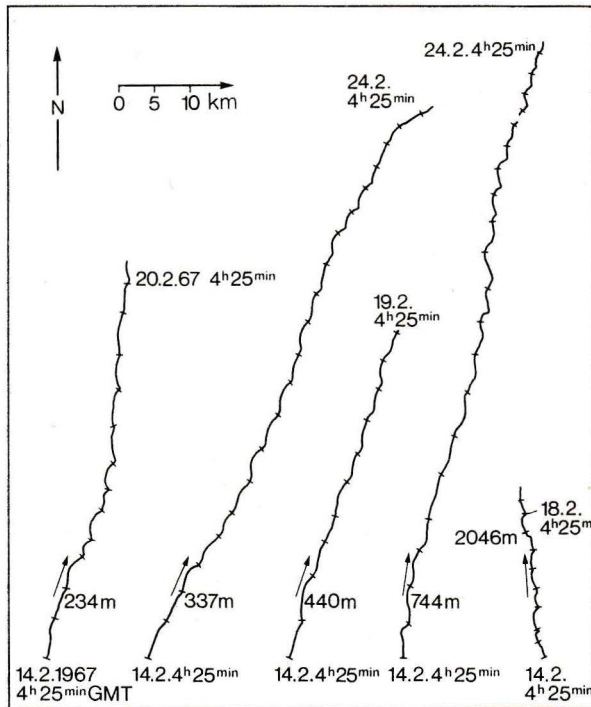


Fig. 4. Progressive vector diagrams. Based on hourly means, bars indicate 12 hourly intervals.

Abb. 4. Progressive Vektor-Diagramme, erstellt aus Stundenmittelwerten. Querstriche kennzeichnen 12-Stunden-Intervalle.

and its magnitude is given for the individual traces. A first inspection of the data indicates a dominating north component of the mean flow, a strong semi-diurnal tidal signal and additional high-frequency variability. The following discussion will deal with these different features of the observed currents.

3 Slowly varying currents

The current variability on time scales larger than semi-diurnal tidal periods is shown by the progressive vector diagrams in fig. 4. They are based on hourly means. At all levels where measurements had been taken, the motion is mainly northward. The directions of the mean currents as given in fig. 5 are parallel to the general direction of the continental margin at this position. The water therefore moves opposite to the mean surface currents of the main North Atlantic gyre, with the Portugal and the Canary Currents in its eastern part. The variability of direction in this slope countercurrent on the above time scales was found to be very small. Typical changes were below 20° during the period of observation. A turn to the left by 10 to 20° is detected in the record from 234 m depth on February 18, 1967. The time of this directional change may be correlated to a sudden

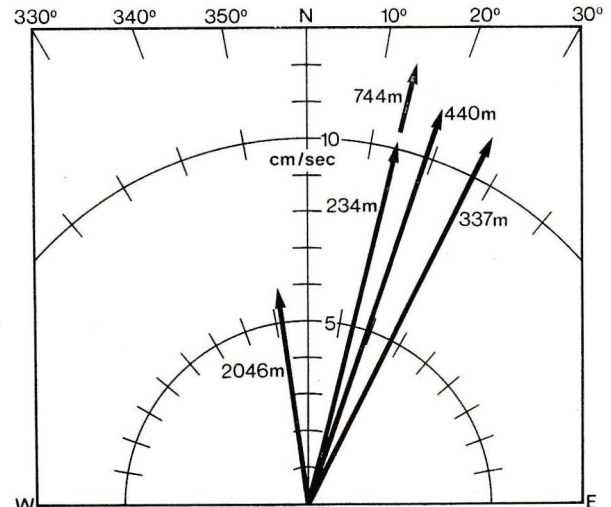


Fig. 5. Mean currents for common record length (see fig. 3).

Abb. 5. Mittlere Ströme für die Zeit der gemeinsamen Registrierung (s. Fig. 3).

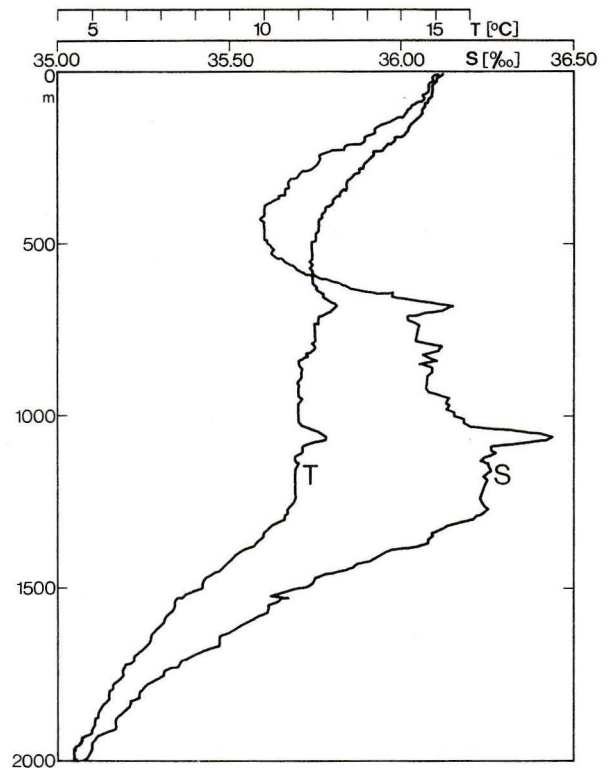


Fig. 6. Typical temperature (T) and salinity (S) profiles on station no. 8065 (measurement no. 5, 14 February 1967, 16.05 GMT).

Abb. 6. Typische Temperatur (T)- und Salzgehalts (S)-Profile auf Station Nr. 8065 (Messung Nr. 5, 14. Februar 1967, 16.05 MGZ).

Table 2 Results from the harmonic analysis of currents for a 12.4 hour period. Common record length 115 hours, phases and times referring to moon's transit at Greenwich on February 14, 1967, 03 h 29 min GMT. Negative sign on minor axis of current ellipse indicates clockwise rotation of current vector.

Instr. No.	Depth m	East component			North component			Current ellipse			σ h
		A cm/sec	Φ degr.	noise cm/sec	A cm/sec	Φ degr.	noise cm/sec	LA cm/sec	SA cm/sec	χ degr.	
026101	234	2.7	230	0.5	3.8	115	0.7	4.1	-2.3	155	9.7
026102	337	2.5	227	0.5	3.6	105	0.7	3.9	-1.9	153	9.3
026103	440	2.4	256	0.4	1.9	168	0.3	2.8	-1.3	125	10.8
026104	744	3.3	355	0.6	2.5	221	0.5	3.8	-1.5	124	0.4
026106	2046	2.4	194	0.5	4.3	055	0.9	4.7	-1.4	155	7.8

A = Amplitude Φ = Phase LA = major axis SA = minor axis χ = Orientation of major axis in geographical notation σ = time of max. current in accordance with χ .

Tabelle 2 Ergebnisse der harmonischen Analyse von Strömungskomponenten für die M_2 -Gezeitenperiode. Alle Zeiten bezogen auf den Mond-durchgang in Greenwich am 14. Februar 1967, 03 h 29 min MGZ. Negatives Vorzeichen der kleinen Achse der Stromellipse zeigt Rotation des Stromvektors im Uhrzeigersinn an.

decrease in wind speed from Bft 6–8 to Bft 2–3 after strong winds lasting from February 15 to 17.

The depth levels of the current observations were however too deep to explain this change in direction as a direct effect of the decrease of the Ekman current.

The main objective for measuring the currents at this position was to determine the motion of the Mediterranean outflow water. Typical profiles of temperature and salinity in this area are given in fig. 6. The Mediterranean water with two main maxima in the profiles (ZENK 1971) is found at depths between 700 and approximately 1300 m. Unfortunately, the meter in the center of the core at 1045 m did not operate properly, and no record could be obtained. The meter at 744 m, however, delivered data from the upper less intense main maximum of the Mediterranean water. The mean velocities given in fig. 5 lead to the conclusion that the mean speed at this depth is 2 to 3 cm/sec larger than at shallower levels. The Mediterranean water is not only mixing horizontally with the surrounding Atlantic water; it is advected parallel to the coast.

4 Tidal motion

Energy density spectra of horizontal currents were computed for the maximum common record length of 115 hours, starting 03.55, 14. 2. 67. They are shown in fig. 7. The data were averaged to yield 20 minutes intervals, and mean values and linear trends were removed prior to the analysis. The dominant feature of the spectra is the semidiurnal tidal signal. There is no possibility, however, to resolve for lunar and solar tidal constituents. Amplitudes and phases for a period of 12.4 hours obtained from a simple harmonic analysis are given in table 2. Noise levels were estimated by repeating the harmonic analysis at neighbouring frequencies

for the residual time series. Table 2 reveals a considerable baroclinic structure. A formal description of the observed vertical distribution of semidiurnal tidal currents can be given in terms of internal

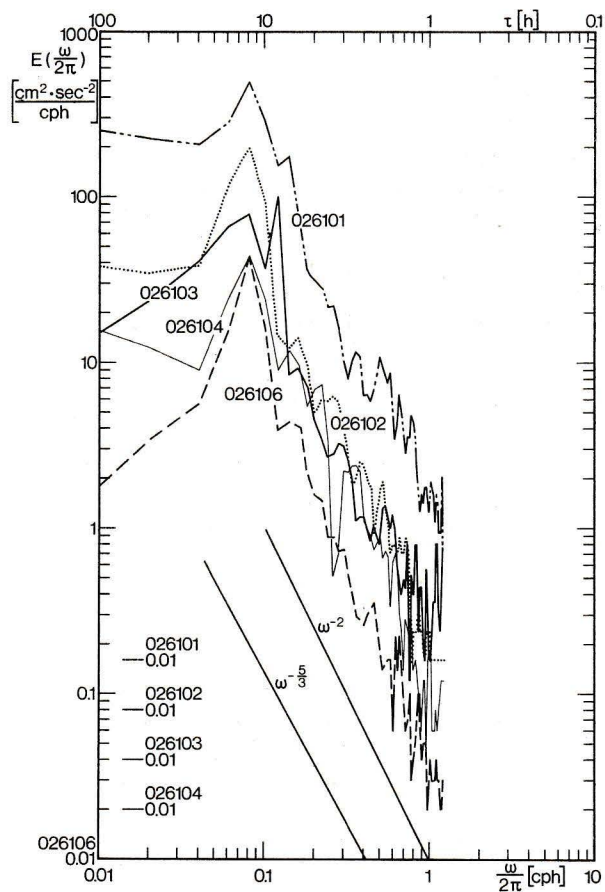


Fig. 7. Energy density spectra of currents. Vertical scale off-set differently for each record, power law slopes indicated by lines below.

Abb. 7. Energiedichtespektren der Ströme. Vertikalskala unterschiedlich verschoben für alle Meßreihen, Potenzgesetzneigungen durch Linien unten angegeben.

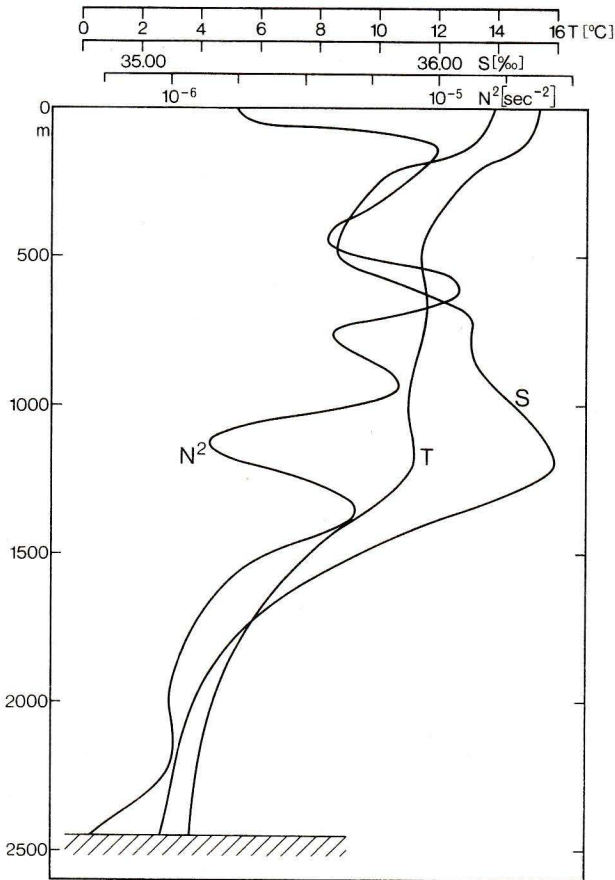


Fig. 8. Mean vertical profiles of temperature (T), salinity (S) and squared Brunt-Väisälä frequency (N) obtained from hydrographic data on station no. 8065.

Abb. 8. Mittlere Vertikalprofile der Temperatur (T), des Salzgehalts (S) und der quadrierten Brunt-Väisälä-Frequenz (N) nach hydrographischen Daten der Station Nr. 8065.

waves using the normal mode approach (see e.g. KRAUSS 1966).

The Brunt-Väisälä frequency distribution given in fig. 8 was computed from hydrographic data obtained during a ten days anchor station of R.V. "Meteor" 5 nautical miles (9 km) north of the mooring site (GIESKES et al. 1970). Eigenfunctions have been computed numerically and were fitted to the observed vertical distribution of Fourier coefficients by the least squares method. Two sets of approximations for the five levels of observation were obtained: In the first case modes of the order zero to two and in the second case modes of the order zero to three were used. Since the use of mode three did not cause significant changes of the lower modes, the results for the second case are presented in table 3 and in figs. 9 and 10.

The largest contribution (48%) to the total kinetic energy of the semidiurnal motion was found with the second order mode. Zero and first order mode contribute 32% and 15% to the kinetic tidal energy content. The smallest portion of only 5% is contributed by the third order mode. Compared to other areas of the North Atlantic Ocean (e.g. GOULD 1973, MAGAARD et al. 1973) where the barotropic or first order baroclinic mode were dominating, the present result is unusual. The intermediate extreme of the second order mode however does coincide with the depth range of the Mediterranean water (see figs. 8 to 10). Thus it is tempting to conclude that the Mediterranean outflow shows stronger tidal fluctuations than the waters above and below.

This conclusion can only be drawn reservedly since the small number of observation levels leaves only one degree of freedom (or two since the use

Table 3 Approximation of the observed vertical distribution of semidiurnal tidal currents by vertical eigenmodes of order 0 to 3. The partition of kinetic energy between modes is given in the last row. Phases referring to moon's transit at Greenwich on February 14, 1967, 03 h 29 min GTM. For symbols and units see table 2.

Tabelle 3 Approximation der beobachteten Vertikalverteilung halbtägiger Gezeitenströme durch Eigenfunktionen der Ordnung 0 bis 3. Die Aufteilung der kinetischen Energie auf die verschiedenen Ordnungen zeigt die letzte Zeile. Phasen bezogen auf den Monddurchgang in Greenwich am 14. Februar 1967, 03 h 29 min MGZ. Erläuterungen der Symbole und Einheiten in Tabelle 2.

Instr. No	Depth	Comp.	Observ.		Mode 0		Mode 1		Mode 2		Mode 3		Modes 0 to 3	
			A	Φ	A	Φ	A	Φ	A	Φ	A	Φ	A	Φ
026101	234	U	2.7	230	0.6	221	1.0	314	2.3	200	0.4	142	2.9	223
		V	3.8	115	2.1	085	2.5	194	2.2	063	0.4	099	3.5	110
026102	337	U	2.5	227	0.6	221	1.0	314	1.4	200	0.4	322	2.2	250
		V	3.6	105	2.1	085	2.4	194	1.3	063	0.4	279	2.8	122
026103	440	U	2.4	296	0.6	221	0.9	314	0.5	200	0.9	322	2.2	282
		V	1.9	168	2.1	085	2.2	194	0.5	063	1.0	379	1.9	145
026104	744	U	3.3	355	0.6	221	0.4	314	3.1	020	0.9	322	3.4	356
		V	2.5	221	2.1	085	0.9	194	2.9	243	1.0	279	2.5	221
026106	2046	U	2.4	194	0.6	221	0.6	134	1.7	200	0.3	322	2.4	194
		V	4.3	055	2.1	085	1.6	013	1.6	063	0.4	279	4.3	055
Vertically integrated kinetic energy (%)					32	15	48	5	100					

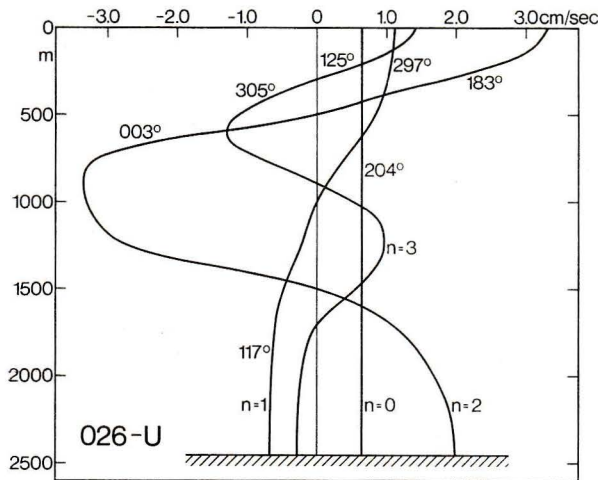


Fig. 9. Modes for order (n) zero to three fitted to the east-west (u) component data.

Abb. 9. Eigenfunktionsanpassung der Ordnung (n) null bis drei für die Ost-West (u)-Komponenten.

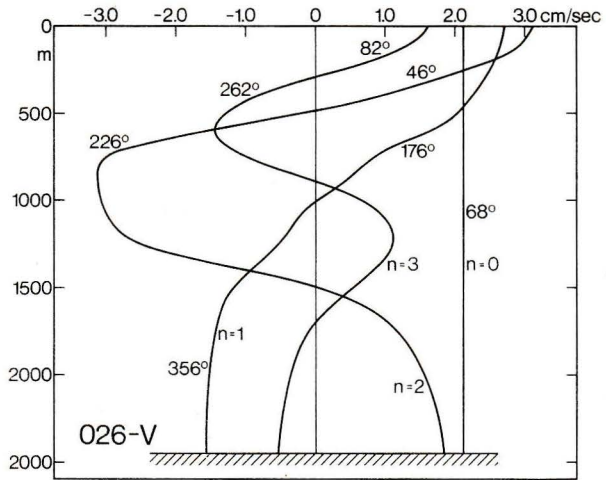


Fig. 10. Modes of order (n) zero to three fitted to the north-south (v) component data.

Abb. 10. Eigenfunktionsanpassung der Ordnung (n) null bis drei für die Nord-Süd (v)-Komponenten.

Table 4 Elements of tidal ellipses for observed and approximated currents at a depth of 234 m. Symbols, units and times as given in table 2.

Tabelle 4 Elemente der Gezeitenstromellipsen der beobachteten und approximierten Strömung im Tiefenniveau 234 m. Symbole, Einheiten und Zeiten wie in Tabelle 2 angegeben.

LA	SA	ζ	σ	LA	SA	ζ	σ
Observation				Mode 0			
4.3	-2.3	155	9.7	2.1	-0.4	168	9.1
Mode 1				Mode 2			
2.6	-0.8	168	0.3	3.0	-1.2	133	7.6
Mode 3				Modes 0 to 3			
0.5	-0.2	45	4.2	3.8	-2.4	148	9.2

of modes 0–2 gives the same results) for the approximation. Furthermore, the harmonic analysis could not resolve the lunar and solar constituents. On the other hand, however, the computed amplitudes of any mode do not exceed the observed amplitudes and the highest order mode is very much smaller than the lower modes. This leaves some confidence in the results of the approximation. The results of the mode approximation are also presented as current ellipses in table 4. Assuming the barotropic mode to be a free wave, the direction of the major axis and the phase of maximum current speed are in close agreement with DIETRICH'S (1944) tidal charts. Furthermore, the major axis is parallel to the general direction of the isobaths of the continental slope. This is also true for the results on the first and second order baroclinic

modes. For these two modes, however, which have estimated wave lengths of 106 and 50 km, respectively, the local topography becomes important.

A second approach for describing the observed vertical distribution of semidiurnal currents was tried by computing the fields of characteristics on sections normal and parallel to the general direction of the continental slope (e.g. ZENK 1970). It was the aim to find depth intervals in the vicinity of the mooring site where the characteristics were tangent to the bottom profile. These intervals of "critical slope" are areas of possibly effective interaction between barotropic and baroclinic modes (MOOERS 1972) and thus a possible origin for rays of baroclinic energy propagation. A measurement of energy at the intersection of those rays with the mooring line might be an indication for such a propagation. The result of this second approach, however, was negative since the bottom topography in the vicinity of the mooring site is so complicated (see fig. 1) that areas of critical slope could be defined for any depth in any direction.

5 High frequency motion

The energy density spectra of the current velocities in fig. 7 display a rather steady decrease of the energy levels at high frequencies beyond the semidiurnal peak. The only exception is record 026 103. The high spectral energy at frequencies above 0.5 cph for this series is very probably due to the poor read pulses introducing noise which affects the high frequency signals in the data.

It has been found in other areas of the ocean that the high frequency part of the internal gravity wave spectrum can be described by a power law with $E(\omega) \sim \omega^{-n}$ (WEBSTER 1969, GARRETT et al. 1972, SIEDLER 1974). Here, E is the energy density and ω the circular frequency. Lines indicating $\omega^{-5/3}$ and ω^{-2} are drawn in fig. 7. It appears that the spectra can very well be described by a law $E(\omega) \sim \omega^{-2}$.

Such a law was assumed by GARRETT et al. (1972) to be generally valid in the deep ocean. The spectra from the eastern North Atlantic presented here are consistent with this assumption.

6 Concluding remarks

Mean currents, semidiurnal tidal motions and the slope of energy density spectra for frequencies beyond the tidal range have been presented and conclusions have been drawn in the separate chapters. The authors are aware of the limitations in using the presented data because of the technical problems related to the performance of the current meters, resulting in a poor vertical coverage and in a short period of simultaneous recordings, and because of having data from one location only in an area of highly complicated bottom topography. Despite these limitations it was decided to report on the data and their analyses, since no information from moored instruments had been available before on the Mediterranean outflow at such a distance from the source. It is hoped that especially the result on the baroclinic structure of tidal currents influenced by the Mediterranean water will stimulate further investigations.

Acknowledgements: The help of the crew of R.V. "Meteor" in the mooring deployment is gratefully acknowledged. This work was supported by the Deutsche Forschungsgemeinschaft, Bonn-Bad Godesberg.

References

- CLOSS, H., G. DIETRICH, G. HEMPEL, W. SCHOTT & E. SEIBOLD (1969): „Atlantische Kuppenfahrten 1967“ mit dem Forschungsschiff „Meteor“. Reisebericht. — „Meteor“ Forsch.-Ergebn. A 5: 1–71. Berlin — Stuttgart.
- DIETRICH, G. (1944): Die Schwingungssysteme der halb- und eintägigen Tiden in den Ozeanen. — Veröff. Inst. Meereskd. Berlin, N. F. (A) 41: 1–68.
- GARRETT, C. & W. MUNK (1972): Space-time scales of internal waves. — Geophys. Fluid Dyn. 2: 225–264.
- GIESKES, J. M., J. MEINCKE & A. WENCK (1970): Hydrographische und chemische Beobachtungen auf einer Ankerstation im östlichen Nordatlantischen Ozean. — „Meteor“ Forsch.-Ergebn. A 8: 1–11. Berlin — Stuttgart.
- KRAUSS, W. (1966): Methoden und Ergebnisse der Theoretischen Ozeanographie Bd. 2. — Interne Wellen. 1–248. Berlin.
- MOOERS, C. N. K. (1972): The mixed initial-boundary value problem for inertial-internal waves in a wedge. — Rapp. P.-v. Explor. Mer 162: 57–64.
- SIEDLER, G. (1967): Die Häufigkeitsverteilung von Wasserarten im Ausstrombereich von Meeresstraßen. — Kieler Meeresforsch. 24: 59–65.
- (1974): The fine-structure contamination of vertical velocity spectra in the deep ocean. — Deep-Sea Res. 21: 37–46.
- SIEDLER, G. & E. SEIBOLD (1973): Currents related to sediment transport at the Ibero-Moroccan continental shelf. — „Meteor“ Forsch.-Ergebn. A 14: 1–12. Berlin — Stuttgart.
- WEBSTER, F. (1969): Turbulence spectra in the ocean. — Deep-Sea Res., Suppl. to 16: 357–368.
- ZENK, W. (1970): On the temperature and salinity structure of the Mediterranean water in the North-east Atlantic. — Deep-Sea Res. 17: 627–631.
- (1971): Zur Schichtung des Mittelmeerwassers westlich von Gibraltar. — „Meteor“ Forsch.-Ergebn. A 9: 1–30. Berlin — Stuttgart.

Received July 23, 1974

Revision received September, 1974

Gould, W.J. and W.D. McKee (1973): Vertical structure of semi-diurnal tidal currents in the Bay of Biscay. — *Nature*, **244** (5411), 88–91

Magaard, L. and W.D. McKee (1973): Semi-diurnal tidal currents at "site D". — *Deep-Sea Research*, **20**, 997–1010